

Application of Optimization Techniques for an Optimal Fertilization by Centrifugal Spreading

Teddy Virin^{*}, Jonas Koko[†], Emmanuel Piron^{*}, Philippe Martinet[‡], Michel Berducat[§]

^{*}Cemagref, Montoldre, France

Email: teddy.virin@cemagref.fr

[†]LIMOS, Université de Blaise Pascal, Aubière, France

Email: koko@isima.fr

[‡]LASMEA, Université de Blaise Pascal, Aubière, France

Email: Philippe.MARTINET@lasmea.univ-bpclermont.fr

[§]Cemagref, Aubière, France

Email: michel.berducat@cemagref.fr

Abstract—Mineral fertilizers application is an agricultural task widely performed by centrifugal spreaders. These machines give satisfying results with regularly spaced parallel tractor trajectories but lead to over and under-applications when geometrical singularities occur (non-parallel paths, start and end of spreading,...). The application errors result then in watercourses pollution and important yield losses. In this study, in order to improve fertilizer application by centrifugal spreading, an optimization problem is considered. The optimal parameters are computed by taking into account the mechanical constraints of the machine so that they can be used as reference variables to control the spreader in the future. Faced with a large scale constrained problem, an augmented Lagrangian algorithm using a l-bfgs technique is implemented. The improvements provided by this new method are exposed through simulation results for parallel and non parallel paths in the field.

Index Terms—Optimization, Centrifugal spreading, Augmented lagrangian.

I. INTRODUCTION

Fertilization practice is an important agricultural operation which consists in applying nutrients within arable land in order to make up the soil deficiencies and thus permit a correct growth of the plants. This task is above all performed by centrifugal spreaders which are machines famous for their low cost and their simplicity of use. Unfortunately, because of an unsuitable strategy, centrifugal spreading often results in harmful environmental effects. Indeed, an over-application in some spots mostly results in an over nitrate enrichment and with ground lixiviation, can cause problems of excessive growth of algae in surface waters. This phenomenon known as eutrophication lead then to numerous aquatic animals disappearances [1]. In case of under-application, yield losses can be very important. Consequently in order to limit groundwaters and watercourses pollution by fertilization, european and american governments were led to impose strict rules as in [2]. Faced with these requirements, investigations are more and more carried out to improve the quality of the distribution achieved by centrifugal spreaders. Here, an approach for optimization of fertilizer application during spreading is presented. We consider an optimization problem based upon the actual spatial

distribution model developed in [3] and in [4], instead of using the traditional method relied on the best arrangement of the transverse distribution. Moreover, thanks to this strategy, spreader mechanical constraints can be considered and thus the solutions of the problem may be used as reference values for the control of the machine. In this study, only optimization along trajectories in the main field body is considered and not in the boundaries zones of the farmland. This paper is organized as follows. In section II, the centrifugal spreading process and the related application errors are dealt with. The cost function and its discretization are exposed in section III. Faced with a large scale problem, we present a decomposition of the problem and the applied algorithm in section IV. In section V, optimization results are illustrated for parallel and non parallel tractor trajectories in the main field body.

II. PROBLEM STATEMENT

The main spreading aim is to obtain an amount of actually distributed fertilizers close to a prescribed dose determined from agronomical and pedological considerations. This regularity is essentially achieved by centrifugal spreaders with double spinning discs, represented in Fig.1. While the tractor progresses within the farmland along tramlines, fertilizers granulars contained in the hopper of the spreader pour onto each rotating disc and are ejected by centrifugal effect. Usually, thanks to a GPS antenna and a radar speed sensor, location and speed of tractor are known. Then, according



Fig. 1. Centrifugal spreader with double spinning disc during fertilization practice

to these parameters and a prescribed application map previously defined, an actuator, permitting to change flow rates, is controlled. The amount of applied fertilizers, currently called spread pattern, has an irregular distribution which is often highlighted by a transverse distribution curve obtained from the summation of all the amounts deposited along each travel direction. An example of spread pattern and its transverse distribution are illustrated in Fig.2. As depicted in Fig.3, this spatial distribution heterogeneity leads then the tractor driver to follow outward and return paths in order to obtain an uniform deposit from transverse distributions summation for each successive travels within the field.

Nowadays, fertilization strategy is based above all upon the best overlappings of the transverse distributions with respect to the different tractor paths. Indeed most of the experiments and simulations undertaken in order to assess fertilizer application accuracy or study device settings are only carried out by using this method as specified in test procedures defined by [5]. So, for example, this procedure is used to explain how to adjust spreaders settings to have better application uniformity and can be also applied to outline the performance and the defects of machines like in [6]. Usually, a regular dose is achieved when the distance between two consecutive overlapping lines, currently called working width, is equal to the distance separating two successive tramlines. Besides, these overlapping lines correspond to symmetry axis which make two successive paths coincide. It is also important to notice that the mass flow rates permitting to check these conditions are calculated thanks to a simple mathematical expression given by:

$$m = (Q^* \cdot W \cdot S) / 600 \quad (1)$$

where m is the mass flow rate (Kg/min), Q^* the desired dose (Kg/Ha), W the working width (m) and S the speed of tractor (Km/h). When computing this relation, we reason as if fertilizers were homogeneously applied onto a rectangular area which length is equal to the wished working width. Unfortunately, in this case, the actual phenomenon occurring during spreading process is completely ignored. Indeed, the

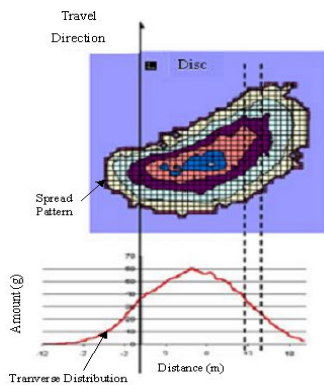


Fig. 2. Spread pattern (spatial distribution) and transverse distribution (red curve)

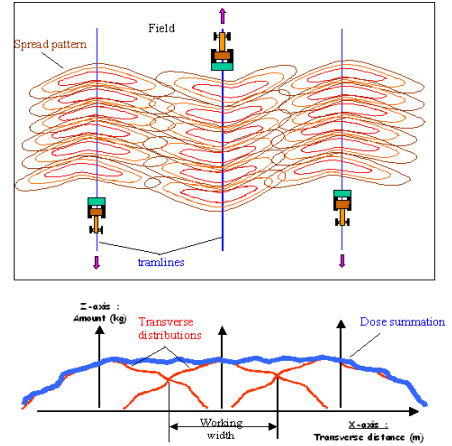


Fig. 3. Fertilization strategy based upon transverse distribution summation.

true global deposit of nutrients in the farmland is due to spread pattern overlappings and thus is the result of the heterogeneous spatial distribution summation at each position of the spreader. So, this method can give some very satisfying results as long as tramlines are parallel and regularly spaced but is inefficient if the field presents some geometrical singularities such as non parallel paths, irregularly spaced parallel paths, start and end of spreading... Then, in these spots, some local application errors occur, as shown in Fig.4. These fertilization errors can also reach an absolute value close to 95% which can cause serious environmental and economic issues. In view of the efficiency enabled by a pre-planning of the trajectories shown by [7], a first solution to enhance application accuracy could be to search optimal paths for the implement. Therefore, some works were done about tractor paths optimization with respect to the considered agricultural operation like in [8]. However these methods cannot be applied when trajectories are already fixed by other agricultural task like sowing for example. Consequently, it is very important to know how best arrange the shape and the placement of the actual spatial distributions, that is to say spread pattern, during spreading process according to the imposed geometrical constraints met in the arable land. This adjustment should be continuously carried out for each GPS position of the spreader by changing its settings. Thus, in this study, we focus on a method which calculates optimal parameters permitting to obtain best spread pattern arrangement in the presence of imposed paths.

III. PROBLEM MODELLING

Let us first precise some notations. The distributed dose model needs the definition of some geometrical and temporal parameters described by:

- $\Omega \in \mathbb{R}^2$, polygonal domain (field),
- $t \in \mathbb{R}$, time,
- $s(t) \in \mathbb{R}^2$, path in Ω ,
- $x \in \Omega$, coordinates of points
- $r(x, t) \in \mathbb{R}$, distance between $\overrightarrow{s(t)}$ and x ,
- $\theta(x, t) \in \mathbb{R}$, angle between $\overrightarrow{s(t)}$ and x .

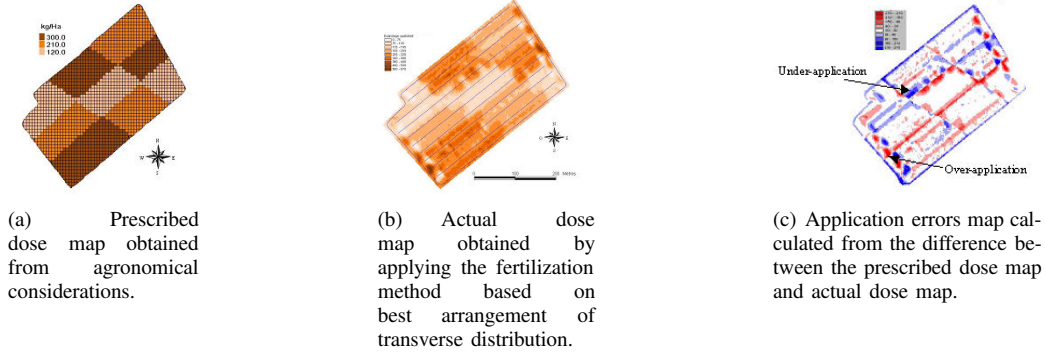


Fig. 4. Application errors resulting from the reasoning based on the best transverse distribution investigation and not on spread patterns overlappings.

The spread pattern model depicted in Fig.2 is often described by using its medium radius and medium angle. The medium radius defines the distance between the disc centre and the spread pattern centre while the medium angle corresponds to the angle between the travel direction and the straight line passing through the disc centre and the spatial distribution one. These variables are given by:

$$\begin{aligned}
m(t) &\in \mathbb{R}, & \text{mass flow rate for right disc,} \\
d(t) &\in \mathbb{R}, & \text{mass flow rate for left disc,} \\
\rho(t) &\in \mathbb{R}, & \text{medium radius for right disc,} \\
\xi(t) &\in \mathbb{R}, & \text{medium radius for left disc,} \\
\varphi(t) &\in \mathbb{R}, & \text{medium angle for right disc,} \\
\psi(t) &\in \mathbb{R}, & \text{medium angle for left disc.}
\end{aligned}$$

We define also σ_r and σ_θ the standard deviations for the radius and the angle respectively which are supposed to be constant. Then according to the simplifying assumptions and statistics tests considered by [3] and [4], the radial and angular distributions of the spread pattern are very close to normal distributions. Thus, the spread pattern ejected by the right and left discs are respectively $q_r \in \mathbb{R}^2$ and $q_l \in \mathbb{R}^2$ and given by:

$$q_r(x, m(t), \rho(t), \varphi(t)) = \tau \cdot \exp(-(r(x, t) - \rho(t))^2/a) \cdot \exp(-(\theta(x, t) - \varphi(t))^2/b) \quad (2)$$

$$q_l(x, d(t), \xi(t), \psi(t)) = \kappa \cdot \exp(-(r(x, t) - \xi(t))^2/a) \cdot \exp(-(\theta(x, t) - \psi(t))^2/b) \quad (3)$$

where $a = 2\sigma_r^2$, $b = 2\sigma_\theta^2$, $\tau = m(t)/(2\pi\sigma_r\sigma_\theta)$ and $\kappa = d(t)/(2\pi\sigma_r\sigma_\theta)$. To simplify notations, we define $M(t) = (m(t), d(t)) \in \mathbb{R}^2$, $R(t) = (\rho(t), \xi(t)) \in \mathbb{R}^2$ and $\Phi(t) = (\varphi(t), \psi(t)) \in \mathbb{R}^2$. The total spatial distribution q_{tot} is then:

$$q_{tot}(x, M(t), R(t), \Phi(t)) = q_r(x, m(t), \rho(t), \varphi(t)) + q_l(x, d(t), \xi(t), \psi(t)) \quad (4)$$

From this model, the actual distributed dose $Q \in \mathbb{R}^2$ during the interval of time $(0, T)$ for single tramline can be calculated as:

$$Q(x, M, R, \Phi) = \int_0^T q_{tot}(x, M(t), R(t), \Phi(t)) dt \quad (5)$$

Here, in order to reduce harmful fertilization effects, it is imperative to minimize the difference between the actual dose

and the desired dose. If $Q^* \in \mathbb{R}^2$ is the prescribed dose, the objective is thus to determine the optimal functions M , R and Φ so that they minimize the following functional:

$$F(M, R, \Phi) = \int_{\Omega} [Q(x, M, R, \Phi) - Q^*]^2 dx \quad (6)$$

where Q^* is the desired application rate. (6) cannot be analytically evaluated. This statement lead to discretize the functional F and use an approximative integration method. A spatial discretization is performed by introducing a grid of Ω so that Q and Q^* are afterwards calculated by considering bilinear approximations. Moreover, let us divide the interval $(0, T)$ into n elements with equal length $\delta = T/n$. We can then define $t_j = j\delta$ with $j = 0, 1, \dots, n$. Consequently, we can assume $M_j = M(t_j)$, $R_j = R(t_j)$ and $\Phi_j = \Phi(t_j)$. The corresponding vectors are given by:

$$M = \begin{bmatrix} M_0 \\ \vdots \\ M_n \end{bmatrix}, \quad R = \begin{bmatrix} R_0 \\ \vdots \\ R_n \end{bmatrix}, \quad \Phi = \begin{bmatrix} \Phi_0 \\ \vdots \\ \Phi_n \end{bmatrix}.$$

In order to take into account the mechanical limits of the system and not to untimely solicit actuators, the functions M , R and Φ and their time derivative are subject to bound constraints. The set of solutions is then defined by $S = \{(M, R, \Phi) \in \mathbb{R}^{6(n+1)}\}$ so that:

$$\begin{cases} M_{min} \leq M \leq M_{max} \\ R_{min} \leq R \leq R_{max} \\ \Phi_{min} \leq \Phi \leq \Phi_{max} \\ |M_{i+1} - M_i| \leq \alpha\delta \\ |R_{i+1} - R_i| \leq \beta\delta \\ |\Phi_{i+1} - \Phi_i| \leq \gamma\delta, \end{cases} \quad (7)$$

where $|\cdot|$ stands for the classical absolute value and α , β and γ are known parameters fixed with respect to the machine mechanical characteristics. Consequently, the nonlinear programming problem which has to be considered is given by:

$$(P) \quad \min_{(M, R, \Phi) \in S} F(M, R, \Phi) \quad (8)$$

The set S is a bounded closed, then it is a compact set in $\mathbb{R}^{6(n+1)}$. Therefore, the problem (P) has at least one local

minimum. In most cases, the field contains several tramlines and then the true distributed dose is the result of the summation of the applied dose for each indexed k tractor trajectory. If we assume that w is the number of tramlines and that each path $s^k(t)$ is defined in the interval (t_i^k, t_f^k) , the actual distributed dose can be calculated as:

$$Q(x, M, R, \Phi) = \sum_{k=1}^w \int_{t_i^k}^{t_f^k} q_{tot}(x, M(t), R(t), \Phi(t)) dt \quad (9)$$

Therefore, if we define also $M_j^k = M(t_j^k)$, $R_j^k = R(t_j^k)$, $\Phi_j^k = \Phi(t_j^k)$, we can apply the same discretization scheme as before. Usually, the tractor follows more than five tramlines in the field. These ones have often a length superior to one hundred meters. Then, it is clear that discretization generates an optimization problem with numerous variables. Thus, this statement lead us to decompose the problem as it is explained in the next section.

IV. PROBLEM DECOMPOSITION

In most cases, prescribed dose maps illustrated in Fig.4(a) are 1 m-gridded. For practical reasons, we use the same spatial grid for discretization. In order to lose informations as little as possible, the temporal discretization is carried out so that we compute two samples of each parameters per cell. If we consider only three paths which length is equal to one hundred meters within the field, the number of parameters raises then to 3600. It is obvious that this large scale problem cannot be solved directly by an optimization algorithm in view of the high computational time which would be caused. Faced with this difficulty, we decompose the problem (\mathcal{P}) into sub-problems so that each trajectory is individually dealt with. Then, the domain Ω is decomposed into w subdomains where w is the number of paths. Therefore, let us define the following notations:

$$\begin{aligned} K_1 &= \{k \in \mathbb{N} | 1 \leq k \leq w\}, \\ K_2 &= \{k \in \mathbb{N} | 1 \leq k \leq w-1\}, \\ K_3 &= \{k \in \mathbb{N} | 2 \leq k \leq w\}, \\ L_1 &= \{l \in \mathbb{N} | \forall z \geq 2 \in \mathbb{N}, 1 \leq l \leq z\}, \\ L_2 &= \{l \in \mathbb{N} | \forall z \geq 2 \in \mathbb{N}, 2 \leq l \leq z\}, \\ \Omega &= \bigcup_{k \in K_1} \Omega^k, \quad \Omega^k = \bigcup_{l \in L_1} \Omega_l^k, \end{aligned}$$

with $\Omega^k \in \mathbb{R}^2$ the k^{th} subdomain of Ω , and $\Omega_l^k \in \mathbb{R}^2$ the l^{th} subdomain of Ω^k . In order to consider separately each trajectory $s^k(t)$, the subdomains Ω^k are defined so that:

$$\begin{cases} \partial\Omega^k \cap \Omega^{k+1} = s^{k+1}(t), \quad \forall k \in K_2 \text{ and } \forall t \in (t_i^{k+1}, t_f^{k+1}) \\ \partial\Omega^k \cap \Omega^{k-1} = s^{k-1}(t), \quad \forall k \in K_3 \text{ and } \forall t \in (t_i^{k-1}, t_f^{k-1}) \end{cases}$$

In order to make easier to understand the spatial decomposition, Fig.5 illustrates the example of three parallel tramlines in a domain Ω with a rectangular geometry. Furthermore, $\forall (l, k) \in L_1 \times K_1$, we define I_l^k and v_l^k so that $I_l^k = \{i \in \mathbb{N} | q_{tot}(x, M_i^k, R_i^k, \Phi_i^k) \neq 0 \forall x \in \Omega_l^k\}$ and $v_l^k = \text{card}(I_l^k)$. If we assume that M_l^k , R_l^k and Φ_l^k are $v_l^k \times 1$ matrices such as $(M_l^k)_i = M_{i \in I_l^k}^k$, $(R_l^k)_i = R_{i \in I_l^k}^k$ and $(\Phi_l^k)_i = \Phi_{i \in I_l^k}^k$, we can then define as previously the set of

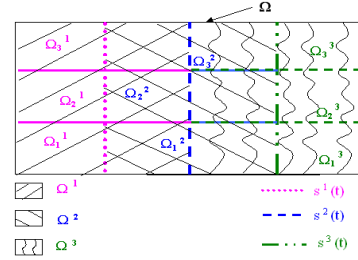


Fig. 5. Rectangular domain Ω divided into 9 subdomains Ω_l^k , $1 \leq l \leq 3$, $1 \leq k \leq 3$.

constraints $S_l^k = \{(M_l^k, R_l^k, \Phi_l^k) \in \mathbb{R}^{6v_l^k}\} \forall (l, k) \in L_1 \times K_1$ so that:

$$\begin{cases} M_{min} \leq M_l^k \leq M_{max} \\ R_{min} \leq R_l^k \leq R_{max} \\ \Phi_{min} \leq \Phi_l^k \leq \Phi_{max} \\ |M_{i+1}^k - M_i^k| \leq \alpha\delta \\ |R_{i+1}^k - R_i^k| \leq \beta\delta \\ |\Phi_{i+1}^k - \Phi_i^k| \leq \gamma\delta, \end{cases} \quad (10)$$

We can now define, as done in the previous section, the variables $M_l^k \in \mathbb{R}^{2v_l^k}$, $R_l^k \in \mathbb{R}^{2v_l^k}$ and $\Phi_l^k \in \mathbb{R}^{2v_l^k}$ as the respective restriction of M , R and Φ in Ω_l^k . Their dimension v_l^k is determined, according to the temporal discretization technique, as the time from which all distributed dose does not affect the subdomain Ω_l^k . Let us also assume S_l^k be the restriction of the set of constraints S in Ω_l^k . By taking into account the symmetries conditions exposed in section II, the problem (\mathcal{P}') can be defined as the natural decomposition of (\mathcal{P}). The decomposed problem is then obtained as:

$$(\mathcal{P}') \quad \begin{cases} \min \sum_{l=1}^z \sum_{k=1}^w J_l^k(x, M_l^k, R_l^k, \Phi_l^k) \\ (M_l^k, R_l^k, \Phi_l^k) \in S_l^k, \quad (l, k) \in L_1 \times K_1 \end{cases} \quad (11)$$

where

$$J_l^k(x, M_l^k, R_l^k, \Phi_l^k) = \int_{\Omega_l^k} [Q_l^k(x) - Q^*]^2 dx \quad (12)$$

with $Q_l^k(x)$ the actual distributed dose within Ω_l^k taking into account not only the amounts already applied in Ω_l^{k-1} and Ω_{l-1}^k but also the future distributed dose along the path $s^{k+1}(t)$ which is predicted so that it respects the symmetries properties previously explained. Thus, solving the problem (\mathcal{P}') consists in minimizing in a sequential way the application errors in each subdomain by considering what was already distributed before and what will be after. The problem (\mathcal{P}') is an optimization problem subject to inequality constraints. For $(l, k) \in L_1 \times K_1$, to minimize the functional J_l^k we have to consider the following problem:

$$(\mathcal{P}_{ineq}) \quad \begin{cases} \min J_l^k(M_l^k, R_l^k, \Phi_l^k) \\ \min_j \leq h_j(M_l^k, R_l^k, \Phi_l^k) \leq \max_j, \\ j = 1, 2, \dots, 6v_l^k \end{cases} \quad (13)$$

where h_j denotes the j^{th} double inequality, \min_j and \max_j its lower and upper bound. A priori, we do not know which

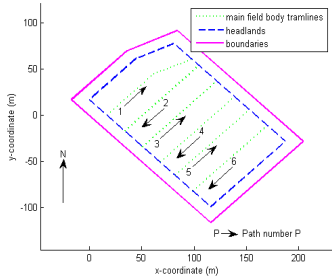


Fig. 6. Field with parallel and non parallel tramlines

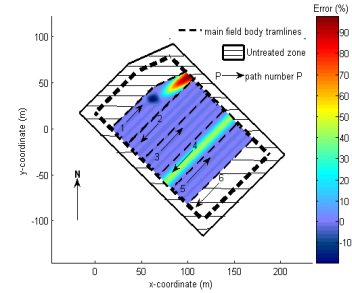


Fig. 7. Application errors obtained with the manufacturers settings

constraints will be saturated for the optimal solution. To avoid this difficulty and have acceptable solution after algorithm execution, we use an augmented lagrangian algorithm, presented in [9], which permits to severely penalize unacceptable parameters. Moreover, in view of the costly computational time caused by the cost function and gradients evaluations, we choose to implement also a l-bfgs technique shown to be efficient in this case by [10]. Then, we obtain the following algorithm:

Step 0: $k = 1, l = 1, X$ in S_1^1 ,

Step 1: if $l \leq z$, minimize J_l^k by using the augmented lagrangian algorithm associated with the L-BFGS minimization technique, otherwise goto **Step 3**,

Step 2: $l \leftarrow l + 1$, goto **Step 1**

Step 3: $k \leftarrow k + 1, X$ in S_1^k , goto **Step 1**.

V. NUMERICAL RESULTS

Here, we are only interesting in optimization within the main field body and not in the boundaries zones where more complex phenomena occur. Besides, a constant prescribed dose fixed at 100 Kg/Ha is considered because even in this case it is difficult to obtain an uniform deposit. The studied field, depicted in Fig.6, presents parallel and non-parallel tramlines. The default distance between parallel trajectories is fixed at 24 m and the tractor speed at 10 Km/h. A narrowing occurs between the paths number 5 and 6 where the distance is equal to 20 m. Furthermore, a non parallel tramline appears for the first path. The average tramlines length is about 100 m. Without optimization, according to tables of rules provided by spreaders manufacturers, settings do not change during spreading process and are only done to have good transverse distributions overlappings for the default working width. This sort of settings permit to obtain results with Matlab environment similar to the ones illustrated in Fig.7. In our case, the used parameters are constant throughout the spreading process $m(t) = d(t) = 15$ Kg/min, $\rho(t) = \xi(t) = 15$ m, $\phi(t) = \psi(t) = 20^\circ$. An over-application area appears at the end of the first tramline and the corresponding error raises to more than 95%. Besides, we can also notice an under-application zone for this path. Because of the narrowing occurring between the 5th and the 6th path, there is also an overdosage at this spot. However, everywhere else the fertilization error is included between -7% and 6% and is

then acceptable. To apply our optimization algorithm, the rectangular subdomains, as achieved in Fig.5, are created so that they are centered on each trajectory and cover the whole main field body. Their size is included between 10 m and 15 m according to geometrical shapes of the arable land. Thus, according to the discretization techniques, the number of computed variables per subdomain evolves between about 370 and 490. The considered mechanical constraints are chosen to gather the characteristics of the most used spreaders. After optimization over the field, we can obtain the results exposed in Fig.8. As we can notice, local application errors are really reduced. The error is included between -9.9% and +6.7%. Over and under-application areas appear above all for the paths number 1 and number 2 because of the geometrical singularity due to the presence of non parallel travel directions. However, this result is very satisfying comparing to fertilization errors previously shown.

As done during spreading process, when consecutive tramlines are completely parallel, parameters are computed so that they are time independent. Consequently, constant parameters are calculated for the paths 3 to 6. Optimal values are gathered in Table I. For the paths 4 and 6, mass flow rates coarsely correspond to the values which would have been calculated by the relation (1). Moreover, in these cases, the other computed values are very close to the ones imposed by the usual settings.

For the two first tramlines, time dependent parameters are evaluated by optimization algorithm. The optimal variables for the path number 1 are presented in Fig.9. In this figure, parameters corresponding to the left and right discs appear respectively on the left and the right. As expected, after the

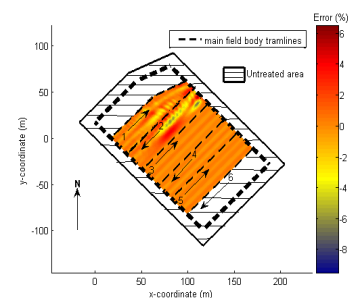


Fig. 8. Application errors obtained after optimization

TABLE I
OPTIMAL VALUES FOR SUCCESSIVE PARALLEL TRAMLINES

Left Disc				
	Path 3	Path 4	Path 5	Path 6
Mass Flow Rate (Kg/min)	20.08	14.95	15.12	20
Medium Radius (m)	15.33	13.34	13.35	15.28
Medium Angle (°)	-19.73	-19.59	-19.43	-19.91
Right Disc				
	Path 3	Path 4	Path 5	Path 6
Mass Flow Rate (Kg/min)	19.9	21.72	21.54	20
Medium Radius (m)	15.31	15.45	15.37	15.28
Medium Angle (°)	19.93	18.24	18.54	19.91

travel direction change, the medium radius drops. Moreover, for the left disc, the mass flow rate evolves little around break-point and seems not to be affected by the occurring narrowing. In return, for the right disc, this parameter increases before the break-point and drops just after this one. Concerning the medium rate angle, we can notice a similar evolution around this point. Fig.10 shows an increasing of all parameters for each disc. This phenomenon can be clearly explained by the narrow pass occuting when the tractor come in the main field body. The values reached after stabilization are close to the ones obtained with 24 m spaced parallel trajectories.

VI. CONCLUSION

In this paper, a new approach for minimization of fertilization errors caused by centrifugal spreading has been exposed. A cost function has been formalized from the spread pattern model studied in previous works. After discretization, a large scale problem has been considered. Given the high computational time caused by the important problem size, we have decomposed spatial and time domains into small domains. We have then shown that the initial problem could be solved by considering its restrictions in each subdomain. In order to take into account the mechanical limits of the spreaders, bound constraints have been introduced. To treat these constraints, an augmented lagrangian algorithm has been implemented. The cost function and gradients evaluation being costly, a l-bfgs technique has been chosen to evaluate the

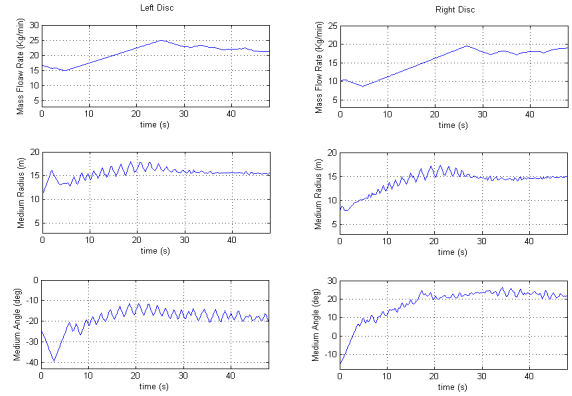


Fig. 10. Optimal parameters for the second path

descent direction. We have applied this method for a field with geometrical singularities which often occur in practice. For a constant desired application rate, we have obtained very satisfying results for optimization in the main field body. The computed optimal parameters respecting mechanical constraints can then be used in the future as reference variables to control centrifugal spreaders. Afterwards, some studies are needed to include optimization within boundaries areas. In these cases, spreaders are equipped with special implements which modify the spread pattern model used here. Therefore, another problem modelling will be necessary. Moreover, new requirements related to field limitations occurring, additional constraints should be considered. At last, with recent advances in agricultural vehicles guidance to follow tramlines, the knowledge of optimal spreader settings should significantly enable to improve fertilizers application accuracy.

REFERENCES

- [1] K. F. Isherwood, *Mineral Fertilizer Use and the Environment*, IFA, Ed. IFA, 1998.
- [2] Bruxelles, "Mise en oeuvre de la directive 91/676/cee - pollution par les nitrates a partir de sources agricoles," 2005. [Online]. Available: http://europa.eu.int/eur-lex/lex/LexUriServ/site/fr/com/2002/com2002_0407fr01.pdf
- [3] R. Olieslagers, "Fertilizer distribution modelling for centrifugal spreader design," Ph.D. dissertation, K.U. Leuven, 1997.
- [4] A. Colin, "Etude du procédé d'épandage centrifuge d'engrais minéraux," Ph.D. dissertation, Université technologique de Compiègne, 1997.
- [5] ISO, *ISO 5690/1 Equipment for distributing fertilizers - Test methods - Part 1: Full width fertilizer distributors*, International Organization for Standardization, Geneva, 1985.
- [6] J. P. Fulton, S. A. Shearer, M. E. Anderson, T. F. Burks, and S. F. Higgins, "Simulated application errors for granular materials for fixed and variable-rate application," in *2000 ASAE Annual International Meeting*, ASAE, Ed., no. 001153, Midwest Express Center, Milwaukee, Wisconsin, July 9-12 2000.
- [7] R. J. Palmer, D. Wild, and K. Runtz, "Improving the efficiency of field operations," *Biosystems Engineering*, vol. 84, pp. 283-288, 2003.
- [8] C. R. Dillon, S. Shearer, J. Fulton, and M. Kanakasabai, "Optimal path nutrient application using variable rate technology," in *Proc. of the Fourth European Conference on Precision Agriculture*, 2003, pp. 171-176.
- [9] D. P. Bertsekas, *Constrained Optimization and Lagrange Multipliers Methods*. New York: Academic Press, 1982.
- [10] R. H. Byrd, J. Nocedal, and R. B. Schnabel, "Representations of quasi-newton matrices and their use in limited memory methods," *Mathematical Programming*, vol. 63, pp. 129-156, 1994.

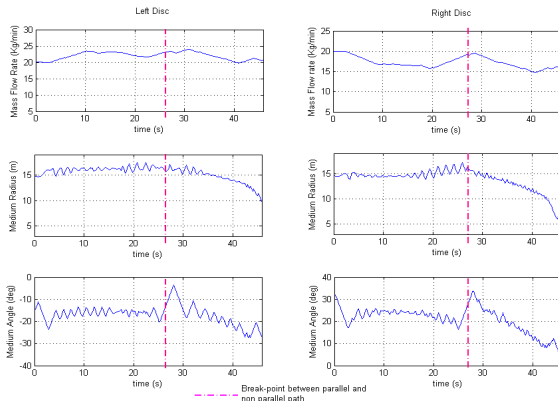


Fig. 9. Optimal parameters for the first path